HHS Public Access

Author manuscript

Neuron. Author manuscript; available in PMC 2017 September 15.

Published in final edited form as:

Neuron. 2017 January 18; 93(2): 362–378. doi:10.1016/j.neuron.2016.11.044.

lncRNA Functional Networks in Oligodendrocytes Reveal Stage-Specific Myelination Control by an *lncOL1*/Suz12 Complex in the CNS

Danyang He[1,2], **Jincheng Wang**[1,5], **Yulan Lu**[3], **Yaqi Deng**[1], **Chuntao Zhao**[1], **Lingli Xu**[1,3], **Yinhuai Chen**[4], **Yueh-Chiang Hu**[4], **Wenhao Zhou**[3], and **Q. Richard Lu**[1,2,3,6]

[1]Divisions of Experimental Hematology and Cancer Biology & Developmental Biology, Department of Pediatrics, Cincinnati Children's Hospital Medical Center, Cincinnati, OH 45229, USA

[2]Integrative Biology Graduate Training Program, University of Texas Southwestern Medical Center, Dallas, TX 75390, USA

[3]Key Laboratory of Birth Defects, Children's Hospital of Fudan University, 201102 Shanghai, China

[4]Division of Developmental Biology, Cincinnati Children's Hospital Medical Center, Cincinnati, OH 45229, USA

[5]Zhejiang Province Key Laboratory of Anti-cancer Drug Research, Institute of Pharmacology and Toxicology, College of Pharmaceutical Sciences, Zhejiang University, 310058 Hangzhou, China

Summary

Long noncoding RNAs (lncRNAs) are emerging as important regulators of cellular functions, but their roles in oligodendrocyte myelination remain undefined. Through de novo transcriptome reconstruction, we establish dynamic expression profiles of lncRNAs at different stages of oligodendrocyte development and uncover a cohort of stage-specific oligodendrocyte-restricted lncRNAs, including a conserved chromatin-associated *lncOL1*. Co-expression network analyses further define the association of distinct oligodendrocyte-expressing lncRNA clusters with protein-coding genes and predict lncRNA functions in oligodendrocyte myelination. Overexpression of *lncOL1* promotes precocious oligodendrocyte differentiation in the developing brain, whereas genetic inactivation of *lncOL1* causes defects in CNS myelination and remyelination following injury. Functional analyses illustrate that *lncOL1* interacts with Suz12, a component of polycomb repressive complex 2, to promote oligodendrocyte maturation, in part, through Suz12-mediated

Correspondence to: Q. Richard Lu.

[6]Lead Contact

Accession Numbers: The accession number for the RNA-seq, ChIP-seq data, and lncRNA annotation reported in this paper is GEO: GSE82211.

Supplemental Information: Supplemental Information includes Supplemental Experimental Procedures and seven figures and can be found with this article online at http://dx.doi.org/10.1016/j.neuron.2016.11.044.

Author Contributions: D.H. and Q.R.L. designed the experiments, analyzed data, and wrote the manuscript with input from all authors. D.H. performed most of the experiments. Y.D. helped with animal surgery. J.W. and C.Z. assisted with biochemical assays, ChIP-seq, and ChIP-qPCR experiments. Y.C. and Y.-C.H. assisted with mutant animal generation. Y.L., L.X., and W.Z. did network construction analysis and provided inputs.

repression of a differentiation inhibitory network that maintains the precursor state. Together, our findings reveal a key lncRNA epigenetic circuitry through interaction with chromatin-modifying complexes in control of CNS myelination and myelin repair.

Graphical abstract

He et al. describe an integrated transcriptional map of lncRNA networks at multiple stages during oligodendrocyte lineage progression and reveal a key lncRNA epigenetic circuitry through interaction with chromatin-modifying complexes in control of CNS myelination and myelin repair.

Introduction

Myelination in the CNS by oligodendrocytes (OLs) is required for rapid propagation of action potentials. Defects in myelin repair impair brain functions and contribute to inherited and acquired neurological diseases, such as leukodystrophies and devastating multiple sclerosis (MS) (Mar and Noetzel, 2010; Trapp et al., 1998). Despite the presence of oligodendrocyte precursor cells (OPCs), myelination fails to proceed in demyelinating lesions in MS patients (Chang et al., 2002). At present, the factors that promote the initiation of OPC differentiation and overcome the block for successful remyelination in demyelinating diseases are poorly defined. OL lineage development can be orchestrated by extrinsic and intrinsic cues and coordination of genetic and epigenetic regulators, including transcription factors, chromatin remodelers, and small non-coding RNAs, that activate the myelinogenic program while suppressing differentiation inhibitory pathways (Emery and Lu, 2015; Zuchero and Barres, 2013).

Both human and mouse genomes encode thousands of long noncoding RNAs (lncRNAs) of greater than 200 nt. These lncRNAs are frequently polyadenylated and transcribed by RNA polymerase II, and have no coding potential (Guttman et al., 2009). lncRNAs have been implicated in the regulation of both normal development (Batista and Chang, 2013; Fatica and Bozzoni, 2014) and diseases (Bhan and Mandal, 2014; Lalevée and Feil, 2015). Recent work points to the critical role of lncRNAs in transcriptional and post-transcriptional control of gene expression, the formation of complexes with epigenetic regulatory machinery, and chromosomal architecture organization (Quinn and Chang, 2016; Rinn and Chang, 2012).

Whether lncRNAs are responsible for OL myelination in a temporally specific manner during development and remyelination is unknown. Although studies have shown expression of lncRNAs during CNS development (Mercer et al., 2010; Ramos et al., 2013) and in OPCs (Dong et al., 2015), a mechanistic understanding of the functions of lncRNAs in myelinogenesis in the CNS remains elusive. Identification and characterization of lncRNAs during OL lineage progression are vital to our full understanding of the mechanisms of myelinogenesis and myelin repair in the CNS.

Herein, we provide the first all-inclusive lncRNA annotation and mapping in mouse OLs at different stages. We profiled dynamic lncRNA expression during OL lineage differentiation by utilizing paired-ended next-generation sequencing of RNA and de novo transcriptome reconstruction. Through gene co-expression network analysis, we defined a group of

lncRNAs that are tightly associated with OL differentiation. Among these, we find that *lncOL1*, an OL-restricted lncRNA, is both crucial and sufficient for OPC differentiation as well as timely initiation of myelination and remyelination in the CNS. Furthermore, we found that *lncOL1* interacts with Suz12 in the PRC2 complex to suppress OL differentiation inhibitory pathways. Collectively, our study provides a comprehensive mapping of lncRNAs in the OL lineage for elucidating the transcriptional and epigenetic regulation of myelinogenesis and demonstrates a critical role of lncRNA-mediated epigenetic regulation for OL differentiation and timely CNS myelination.

Results

Comprehensive De Novo Mapping of lncRNAs during OL Lineage Progression

To gain insights into the functions for lncRNAs during OL development, we first set out to create an all-inclusive high-quality catalog of such transcripts using an ab initio transcriptome reconstruction pipeline (Trapnell et al., 2010) that incorporates evidence of RNA transcripts from a collection of RNA deep-sequencing datasets from primary mouse OPCs and OLs that were differentiated with triiodothyronine (T3) for 1 day (iOL [immature OL]) and 3 days (mOL [maturing OL]) (Figures 1A and S1A, available online). To identify putative lncRNA genes, we selected transcripts that were longer than 200 nucleotides and multiexonic and that did not overlap with protein-coding genes on the same strand. We then removed transcripts with coding-potential assessment (CPAT) scores higher than 0.44, which has been shown to identify noncoding RNAs (Wang et al., 2013). The high stringency annotation revealed 2,392 lncRNA transcripts derived from 1,342 unique gene loci (named as *lncOLs*; Figure 1A). Of these loci, 42% were not found in the Ensembl database (Figure S1B). They are located in intergenic regions or introns of well-defined genes (Figures S1C and S1D).

We next examined the expression patterns of lncOLs over a diverse panel of neural cell types (Zhang et al., 2014), neuronal tissues, and other somatic tissues (Yue et al., 2014). As previously reported (Trapnell et al., 2010), the lncRNAs identified had very little protein-coding potential, as measured by the CPAT algorithm (Figure 1B). Additionally, lncRNA exons were less conserved than protein-coding exons, as shown by Phast-Cons scores (Figure 1C), and their average expression levels were lower than those of protein-coding genes in OL lineage cells (Figure 1D). We observed greater tissue specificity (Ts) of lncRNAs than of protein-coding genes (Figures 1E and S1E), which corroborates the notion that lncRNA expression is highly cell-type specific (Guttman et al., 2009). Such analyses enabled us to identify a cohort of lncRNAs that are highly enriched in OL lineage cells (Figure S1E), including those transcribed from previously reported gene loci (Zhang et al., 2014) (e.g., *lncOL1–3*; Figure S1F), which validates our approach, and previously unidentified lncRNAs from unannotated genomic loci (e.g., *lncOL4–6*; Figure S1G).

lncRNAs Are Dynamically Regulated and Expressed during OL Lineage Progression

To further characterize the *lncRNA* expression pattern, we analyzed transcription start site (TSS) regions for the presence of histone modification marks and transcription factor occupancy. In agreement with previous reports (Derrien et al., 2012), a large majority of the

promoters in the identified lncRNAs were associated with the transcription-activating histone marks H3K4me3 and H3K27ac (Figure S2A). More importantly, whereas lncRNAs evolve rapidly and often lack orthologs in other species (Diederichs, 2014), we found that a significant portion of lncOLs is also present in the syntenic loci of rat OL lineage cells, evident by the enrichment of H3K4me3 and H3K27ac in conserved genomic regions (Figures 1F and 1G), suggesting a functionally conserved role of these lncRNAs during OL development. In addition, genomic occupancy by Sox10, an OL-differentiation regulator (Lopez-Anido et al., 2015), was detected at many putative lncRNA promoters in rat OLs (Figures 1F and 1G), suggesting that Sox10 transcriptionally regulates these lncRNAs.

By investigating the dynamics of lncRNA expression over the course of OPC differentiation and maturation, we identified a subset of lncRNAs that were differentially expressed between differentiating OLs and OPCs (Figure 1H). Furthermore, profiling analysis of lncRNA expression after contusive spinal cord injury in mice (Chen et al., 2013) revealed that expression of a group of *lncOL*s, such as *lncOL1*, was reduced at 2 days post-lesion (dpl) and reactivated at 7 dpl during the regeneration process in the spinal cord (Figures S2B and S2C), suggesting a potential importance of lncRNAs for OL regeneration, which diminishes during OL loss and conversely increases during differentiation.

Co-expression Networks between lncRNAs and Protein-Coding Genes in OLs

Expression of many lncRNAs is highly correlated with that of their protein-coding neighbors, and some lncRNAs influence the expression of nearby genes (Rinn and Chang, 2012). However, Pearson coefficient estimation of neighboring pairs of lncRNAs and mRNAs revealed no obvious correlations, as a group, between the majority of *lncOL*s and adjacent mRNAs in the OL lineage (Figures S2D and S2E). This suggests that expression of the majority of *lncOL*s is not related to local transcriptional activity of neighboring protein-coding genes or involved in the same biological processes.

To assess the potential functions of lncOLs, we evaluated the co-relationship between lncOLs and protein-coding genes using the Markov clustering algorithm (MCL), which assigns genes into modules based on their similarity in expression patterns (van Dongen and Abreu-Goodger, 2012). We identified 19 clusters contained at least 100 correlated lncRNAs and protein-coding genes (Figure 1I) that are associated with known biological processes. The lncRNA genes in MCL cluster I are primarily associated with neurogenesis and gliogenesis (Figure 1J). Assessment of the Pearson correlation between lncRNA and protein-coding genes within MCL cluster I revealed that this group of lncRNAs (e.g., *lncOL1* and *lncOL4*) is highly correlated with the myelinogenic gene program, such as *Mbp* and *Nkx2.2* (Figures 1K and S2F), suggesting that this group of lncRNAs is likely involved in OL myelination.

Functional Characterization of OL-Enriched lncOLs in OPC Differentiation

Given that OL-enriched lncOLs were identified in our lncRNA de novo reconstruction and network analysis, we next sought to validate and characterize the expression and function of candidate lncOLs. We selected four lncRNAs from the cluster I lncRNA set for further analysis: *lncOL1–3*, three previously annotated but uncharacterized lncRNAs, and *lncOL4*, a

previously unannotated lncRNA (Figure 2A). *LncOL1–4* are transcribed from genomic regions associated with active histone marks, including H3K4me4 and H3K27Ac (Figure 2A). Despite cellular abundance to various extents, *lncOL1–4* were robustly expressed in mouse CNS tissues, such as the brain and spinal cord, but were barely detectable in other somatic tissues (Figure 2B). Furthermore, concurrent with dynamic expression of OL differentiation regulators, such as Tcf7l2/Tcf4 (Zhao et al., 2016), in the developing spinal cord, *lncOL1–4* expression was detected at the neonatal stage postnatal day (P)0 and peaked at the perinatal stage P14, followed by a sharp decline in adulthood (Figure 2C). Consistently, *lncOL1–4* were substantially upregulated during OPC differentiation in vitro (Figure 2D).

To determine *lncOL1–4* function in OL differentiation, we attenuated their expression in primary OPCs using small interfering RNAs (siRNAs). Knockdown of *lncOL1–4* individually inhibited expression of myelin genes, including *Mbp*, *Plp1*, and *Cnp* (Figures 2E and 2F), suggesting that induction of these lncRNAs is critical for proper OL differentiation in vitro. Next, we investigated whether the gain of function of *lncOL1–4* could promote OL differentiation gene expression. To ensure proper processing and secondary structure formation, we cloned murine *lncOL1–4* into the pBI-CMV3 vector to allow transcription of lncRNAs and a GFP reporter ZsGreen1 from constitutively active bidirectional human cytomegalovirus promoters (Figure 2G). Forced expression of *lncOL1*, *lncOL2*, and *lncOL4* led to a significant induction of differentiation-associated genes (e.g., *Mbp*, *Mag*, and *Myrf*), whereas *lncOL3* exhibited minimal effects on promoting the OL differentiation program (Figure 2G).

LncOL1 Is an OL-Restricted lncRNA that Promotes OL Differentiation In Vivo

Our ranking of oligodendrocytic lncRNAs by their abundance, regulation during the transition from OPC to OL, and potential functions identified *lncOL1* as a top candidate modulator of OL differentiation. Analysis with the various coding-potential assessment tools, including CPAT (Wang et al., 2013), the Coding Potential Calculator (Kong et al., 2007), and PhyloCSF (Lin et al., 2011), indicated that the *lncOL1* transcript has minimal, if any, protein-coding potential (Figure S3A).

In mouse and rat OL lineage cells, *lncOL1* is located within the second intron of *Pcdh17* and is actively transcribed in the direction opposite to *Pcdh17* (Figure 3A). Peaks in genomic occupancy by Sox10 and Olig2, two critical OL transcriptional regulators, were observed near the *lncOL1* TSS in rat OLs. Occupancy of activating histone marks H3K4me3 and H3K27ac as well as Olig2 was markedly enhanced around the TSS of *lncOL1* in differentiating OLs relative to OPCs (Figure 3A), suggesting greater chromatin accessibility and transcription activity at the *lncOL1* promoter during OL differentiation. *lncOL1* expression is restricted to OL lineage cells because transcripts of *lncOL1* were not detected in other neural cell types, such as neural progenitor cells and astrocytes (Figure 3A). In addition, human brain tissues and glioma cells, but no other tissue types, exhibited an enrichment of active promoter-associated H3K4me3 on the predicted TSS of the putative human *lncOL1*, indicating potentially conserved expression of *lncOL1* in the human brain (Figure S3B).

In line with the enhancement of activating histone marks at the *lncOL1* promoter, *lncOL1* transcript levels were substantially induced during OL differentiation, along with *Mbp* and *Myrf* in culture (Figure 3B). In situ hybridization revealed prominent expression of *lncOL1* in CNS white matter tracts in the brain and spinal cord of mice at perinatal stages (Figures 3C and 3D). *lncOL1* was expressed exclusively in a subset of Olig2$^+$ OL lineage cells (Figure 3E). Moreover, *lncOL1* was co-expressed in cells that expressed the mature OL markers CC1 and Sip1/Zeb2 (Weng et al., 2012) (Figure 3E), but was barely detected in PDGFRα$^+$ OPCs (Figure 3E). Taken together, our data indicate that *lncOL1*, an evolutionally conserved lncRNA, is restricted to differentiating OLs in the OL lineage (Figure S3C).

RNA fluorescence in situ hybridization (FISH) showed that *lncOL1* transcripts were detected in both the cytoplasm and nucleus of OPCs, but were enriched in the nuclear fraction and formed multiple “foci” in the nucleus of differentiating OLs (Figure 3F). Consistently, cell fractionation of oligodendroglial cell line Oli-Neu cells (Ljungberg et al., 1995) followed by qRT-PCR demonstrated that the nuclear fraction of *lncOL1* was associated with chromatin (Figure S3D), suggesting a potential role of the *lncOL1* transcript in transcriptional regulation during OL differentiation.

Given that siRNA-mediated silencing of *lncOL1* significantly inhibited myelin gene expression (Figures 2E and 2F), we then evaluated the functional role of *lncOL1* in OL maturation. We attenuated *lncOL1* expression by transduction of OPCs with a lentiviral vector for expression of small hairpin RNAs (shRNAs) designed to target *lncOL1* (Figure S3E). OPCs with *lncOL1* knockdown exhibited a defect in differentiation into MBP$^+$ OLs (Figures 3G and 3H).

Next, we investigated whether the gain of function of *lncOL1* could promote precocious OL formation in vivo. Electroporation of the *lncOL1*-expressing vector pBI-*lncOL1* carrying a GFP reporter (Figure 3I) into the cortical ventricular zone of developing embryos at E14.5 led to the precocious formation of MBP$^+$ OLs that expressed Olig2 at E17.5 (Figures 3J and 3K), at which stage no MBP$^+$ OLs are observed in the control cortex. These observations suggest that enforced expression of *lncOL1* in neural progenitors induces OL differentiation in the cortex.

Loss of lncOL1 Leads to Defects in OL Differentiation and Myelination Onset In Vivo

To investigate the functional requirement for *lncOL1* in OL development in vivo, we generated *lncOL1*-knockout (KO) mice using CRISPR-Cas9 technology (Doudna and Charpentier, 2014). Two pairs of single guide RNAs (sgRNAs) were designed to delete a 5.7-kb region covering the first four exons of *lncOL1* (Figure 4A). Pups from the F0 generation were screened for indels and confirmed by Sanger sequencing of potential off-target sites. A founder carrying a monoallelic deletion was chosen and back-crossed with wild-type mice for three generations. *lncOL1*-KO mice were born at expected Mendelian ratios from heterozygous intercrosses (Figure 4B). qRT-PCR confirmed the loss of transcripts of *lncOL1*-containing regions targeted for deletion in brain tissues of homozygous mutant mice (Figure 4C). Levels of transcripts containing the 3′ non-deleted regions of *lncOL1* were also substantially downregulated (Figure 4C).

When the developing spinal cords at P1 were analyzed, the percentage of $CC1^+$differentiating OLs among $Olig2^+$ OL lineage cells was significantly lower in *lncOL1*-KO mice than in control littermates (Figures 4D and 4E). Similarly, expression of MBP, amature OL marker, was reduced in the *lncOL1*-KO brain compared to controls (Figures 4F and 4G). In contrast, the total numbers of $PDGFR\alpha^+$ OPCs were comparable between control and *lncOL1*-KO animals (Figure 4H). These observations suggest that *lncOL1* is crucial for timely OPC differentiation, but not their formation. Strikingly, ultrastructural analysis of optic nerves from *lncOL1*-KO mice at the onset of myelination, e.g., P9 showed severe defects in myelinogenesis, with essentially an absence of myelinated axons (Figures 4I and 4K). At postnatal week 3, e.g., P17, the peak period of myelinogenesis, the number of myelinating axons had increased in *lncOL1*-KO mice relative to P9 but was still less than that in control mice (Figures 4J and 4K). Notably, the myelin sheaths (as measured by *g*-ratio, the ratio of the diameter of the axon to the diameter of the axon plus its myelin sheath) were significantly thinner in *lncOL1* mutant optic nerves than in controls (Figure 4L).At adulthood, however, the number of mature OLs and degree of myelination were indistinguishable between adult *lncOL1*-KO and control mice (Figure S4). Collectively, these observations indicate that *lncOL1* regulates the timing of OL differentiation and the onset of myelination, but not myelin maintenance.

To determine whether defects in OL maturation in *lncOL1*-KO animals are cell autonomous due to *lncOL1* deletion, we cultured OPCs isolated from control and *lncOL1*-KO neonates and analyzed their capacity to proliferate and to differentiate in vitro. In the presence of mitogen PDGFAA, *lncOL1*-KO OPCs were able to proliferate as they expressed the proliferative marker Ki67 (Figures 4M and 4N). In contrast to efficient differentiation of control OPCs into CNP^+ and MBP^+ OLs upon treatment with T3, *lncOL1*-KO OPCs exhibited significant deficits in their capacity to differentiate into mature OLs (Figures 4O and 4P), suggesting *lncOL1* null OPCs are intrinsically defective in differentiation and maturation.

LncOL1 Is Critical for Proper OL Remyelination after Demyelination

lncOL1 transcription was reactivated during the subacute phases of spinal cord injury (Figure S2B). We then hypothesized that *lncOL1* might participate in myelin repair. To test this hypothesis, we injected lysolecithin (LPC) into the white matter of adult control and *lncOL1*-KO mice at P60 when the numbers of myelinated axons and myelin morphology were comparable between *lncOL1*-KO and wild-type animals (Figure S4). Focal injection of LPC induces rapid myelin breakdown followed by myelin regeneration (Franklin and Ffrench-Constant, 2008). In normal adult spinal white matter, expression of *lncOL1* was hardly detectable; however, *lncOL1* levels were increased over the course of remyelination following LPC-induced demyelination (Figures 5A–5C).

To determine the potential role of *lncOL1* in OL remyelination, we examined the re-appearance of myelin genes and OLs in the lesion during regeneration processes. At 14 dpl, we observed an increase of myelin genes *Cnp*, *Plp1*, *Mag*, or $CC1^+$ OLs in control animals, whereas expression of these myelin genes and the number of $CC1^+$ OLs were substantially reduced in *lncOL1* mutants (Figures 5D–5G). In contrast, loss of *lncOL1* did not appear to

impair the recruitment of PDGFRα$^+$ OPCs because numbers of OPCs in lesions were comparable between control and *lncOL1* null animals (Figures 5H and 5I). Ultrastructural analysis indicated that there were far fewer myelinated axons in the lesions of *lncOL1*-KO mice than in controls (Figures 5J and 5K). In addition, newly generated myelin sheaths around axons at 14 dpl were substantially thinner in *lncOL1*-KO mutants than in controls (Figure 5L). Thus, these observations suggest that *lncOL1* is crucial for the OL remyelination process, but not OPC formation, in the context of white matter injury.

lncOL1 Interacts with the Suz12/PRC2 Complex to Control OL Differentiation Program

Certain lncRNAs have been shown to regulate gene expression through interactions with specific protein partners (Hajarnis et al., 2015; Maass et al., 2014). To identify potential *lncOL1*-interacting proteins, we adopted a sequence-based RNA-protein interaction prediction algorithm catRAPID (Bellucci et al., 2011) and identified a cohort of candidate *lncOL1*-interacting partners (Figure S5A). Among the candidates was Suz12, a component of polycomb repressive complex 2 (PRC2). PRC2 is an epigenetic regulator that participates in transcriptional repression by catalyzing histone H3 trimethylation (Conway et al., 2015). The canonical PRC2 complex consists of Eed, Suz12, and the histone methyltransferase Ezh2, which is required for PRC2 activity.

To test whether *lncOL1* and Suz12 form a ribonucleoprotein complex, we transiently transfected HEK293T cells with plasmids expressing *lncOL1* RNA and hemagglutinin (HA)-tagged Suz12 and performed RNA immunoprecipitation using an anti-Suz12 antibody. *lncOL1* was present in the Suz12 immunocomplex, but the control, *Gapdh* mRNA, was not (Figure 6A). Furthermore, biotin-labeled full-length *lncOL1* RNA, but not control RNA, robustly enriched Suz12 protein from cell lysates of 293T cells that overexpress Suz12 (Figure 6B). More importantly, the *lncOL1*-Suz12 interaction was further confirmed by pulling down endogenous Suz12 in primary oligodendrocytes and analyzing co-purified RNA by qRT-PCR. *lncOL1* was specifically enriched in Suz12 immunoprecipitates compared to the control RNA (Figure 6C). In addition, we found that Suz12 was precipitated with biotin-labeled *lncOL1*, but not by biotin-labeled control RNA from extracts of oligodendroglial Oli-Neu cells (Figure 6D). Similarly, RNA immunoprecipitation assays indicated that *lncOL1* was enriched in the complex pulled down with Suz12, Eed, and Ezh2 from Oli-neu cells under differentiation conditions (Figure 6E). These protein-RNA interaction studies suggest that *lncOL1* and Suz12/PRC2 form a complex in OLs.

Cooperation of *lncOL1* and Suz12-PRC2 Complex Regulates OPC Differentiation

Suz12 was mainly detected in both PDGFRα$^+$ OPCs and CC1 $^+$ oligodendrocytes in the spinal white matter at P14 (Figure 6F). Intriguingly, whereas Suz12 and Ezh2 protein levels were slightly downregulated during OPC differentiation in vitro, H3K27me3 levels substantially increased as OLs became mature, similar to that of *lncOL1* transcripts (Figure 6G). This observation points to a possible involvement of *lncOL1* and Suz12-mediated gene silencing during OL maturation. To evaluate the functional role of the Suz12-PRC2 complex, we knocked down Suz12 and Eed expression in mouse OPCs using retrovirally expressed shRNAs (Shi et al., 2013) (Figure 6H). Similar to the *lncOL1* -deficient OPCs, cells with Suz12 or Eed silencing exhibited a defect in differentiation into MBP$^+$ OLs

compared to control OPCs upon withdrawal of mitogens (Figures 6I and 6J), indicating that PRC2 integrity is critical for OL maturation in vitro. In addition, selective ablation of the *Ezh2* floxed allele with OL lineage-expressing Olig1-Cre in *Ezh2cKO* mice (*Ezh2*$^{fl/fl}$;*Olig1-Cre*$^{+/-}$) led to a dramatic reduction of CC1^{+} and MBP^{+} OLs and myelinated axons (Figures 6K-6M, S5B, and S5C), with an increase of OPC fraction within the OL lineage, as compared with heterozygous controls (Figure 6M). Consistently, interference of Ezh1/2 enzymatic function by the small molecule inhibitor Unc1999 (Konze et al., 2013) diminished the induction of myelin-associated genes (*Mbp*, *Plp1*, *Mag*, *Cnp,* and *Myrf*) in a dose-dependent manner (Figures S5D and S5E). Together, these data suggest that Suz12-PRC2 activity is required for OPC maturation.

To further investigate the cooperativity between *lncOL1* and Suz12-PRC2 during OL differentiation, we overexpressed *lncOL1* in OPCs in the presence of siRNAs against Suz12 or the Ezh1/2 inhibitor Unc1999. We found that the enhancement of OL differentiation (Figures 6N and 6O) and myelination-associated gene expression (Figures 6P and 6Q) driven by *lncOL1* overexpression were overridden by the loss of Suz12 expression or PRC2 enzymatic activity. These observations suggest that the *lncOL1*-regulated OL differentiation process requires the presence of the Suz12-PRC2 complex.

LncOL1 Acts as a Modulatory Factor for Suz12 to Silence the OPC-Enriched Gene Program during OL Differentiation

To investigate the mechanism underlying *lncOL1* functions in OPC differentiation, we performed transcriptome profiling analysis of gene expression alteration in differentiating OLs between *lncOL1*-KO and control OPCs under differentiation conditions. Nuclear lncRNAs can exert regulatory functions in *cis* or in *trans* during cell differentiation (Ulitsky and Bartel, 2013). *lncOL1* is localized in the second intron of the protein-coding *Pcdh17* gene; however, expression of *Pcdh17* was not significantly correlated with expression of *lncOL1*, whereas *lncOL1* is correlated with the myelin gene *Plp1* (Figures S6A and S6B). Furthermore, *Pcdh17* transcript levels were not affected by *lncOL1* knockdown (Figure S6C), and deletion of the *lncOL1* genomic locus did not influence the expression of *Pcdh17* or other genes within 10 Mb of the *lncOL1* locus (Figures S6D and S6E), indicating that *lncOL1* likely exerts its regulatory functions in *trans*.

Consistent with an impaired OL differentiation phenotype, *lncOL1* deletion caused a reduction in expression of OL-enriched genes (gene module I) and an increase in expression of OPC-enriched genes (gene module II) (Zhang et al., 2014) (Figures 7A and 7B). Intriguingly, promoters of upregulated genes in OPC-enriched module II exhibited lower levels of active histone modifications, such as H3K27ac and H3K4me3 than those in OL-enriched module I (Figure 7C), suggesting that *lncOL1* antagonizes the transcriptional program that maintains OPC state while activating OL differentiation programs. Consistently, gene ontology (GO) analysis revealed that the genes downregulated in *lncOL1* null OLs are associated with myelination, cytoskeletal organization, and glial cell differentiation, whereas genes upregulated in *lncOL1* null cells are linked to cell growth, proliferation, and neurogenesis (Figures 7D and 7E). Furthermore, RT-PCR analysis confirmed a substantial reduction in mRNAs encoding myelin structural markers (e.g., *Mbp*

and *Plp1*), regulators of lipid metabolisms (e.g., *Pik3r3* and *Elovl1*), and proteins involved in cytoskeleton organization (e.g., *Gjc2*, *Tppp*, and *Matp7*) in *lncOL1* null OLs compared to controls (Figure 7F). Intriguingly, we did not observe a substantial increase of OPCs in *lncOL1* mutants (data not shown), suggesting that *lncOL1* ablation does not block but delays the transition from OPC to OL. Thus, these observations indicate that *lncOL1* orchestrates the balance necessary between transcriptional programs to permit OL differentiation.

Given the upregulation of the OPC-associated transcriptional program in the absence of *lncOL1*, we hypothesize that *lncOL1* may cooperate with a Suz12-mediated repressive complex to silence the expression of OPC-enriched genes. Chromatin immunoprecipitation sequencing (ChIP-seq) analyses revealed that Suz12 was essentially excluded from H3K27ac-enriched enhancers and promoters in OPCs (Figure 7G). Furthermore, expression of Suz12-targeted genes was downregulated substantially as compared to those without proximal Suz12 binding in OLs (Figure 7H), suggesting that Suz12 silences the transcription of OPC-enriched genes by deposition of repressive H3K27me3 marks on their enhancers and promoters.

To elucidate whether *lncOL1* influences Suz12 function, we assessed the expression of Suz12-targeted genes in differentiating OLs derived from control and *lncOL1*-KO OPCs. Gene set enrichment analysis (GSEA) demonstrated that the levels of genes targeted by Suz12 were significantly increased in *lncOL1*-KO cells (Figure 7I), suggesting that *lncOL1* loss leads to a general de-repression of Suz12-targeted genes. *lncOL1*-Suz12 target gene sets (genes upregulated in *lncOL1* null cells with promoters occupied by Suz12) are associated with cell growth and proliferation, and their expression is enriched in OPCs (Figure 7J). These include *Igf2*, which encodes insulinlike growth factor 2 that promotes OPC growth and proliferation (Frederick and Wood, 2004; Zhang et al., 2010), *H19*, which is an imprinted lncRNA that promotes progenitor cell proliferation (Ratajczak, 2012), and *Cyp1b1*, which encodes the cytochrome P450 family protein that enhances cell proliferation and tumorigenesis (Mitsui et al., 2015) (Figure 7K). These genes are highly expressed in OPCs, but strongly repressed during OL maturation (Figures S6F and S6G) (Dugas et al., 2006; Zhang et al., 2014), suggesting that their expression maintains OPCs in the precursor state. Furthermore, qRT-PCR analyses indicated that expression of these genes was significantly induced in *lncOL1* null OPCs and in cells in which Suz12 expression was silenced (Figures 7L and 7M). Because *lncOL1* depletion had no effect on PRC2 core subunit expression (Figure S6H), we then asked whether the induction of Suz12-targeted genes in *lncOL1* null OLs is due to alteration of Suz12 recruitment. To test this hypothesis, we performed ChIP followed by qPCR (ChIP-qPCR) for Suz12 in mouse OLs from control and *lncOL1*-deficient mice. Suz12 occupancy was enriched at the promoter of *Igf2*, *H19*, and *Cyp1b1* in OLs (Figure S6I). However, it was markedly reduced in the absence of *lncOL1* (Figure 7N), suggesting that *lncOL1* is crucial for Suz12 recruitment on the targeted promoters in OLs. Collectively, these observations indicate that *lncOL1* interacts with Suz12 to promote OL differentiation by promoting the deposition of Suz12 at its targeted gene loci.

Discussion

Dynamic Landscape and Functional Networks of lncRNAs during OL Lineage Progression

Decoding regulatory elements and factors that control OL myelination is important for identifying new therapeutic targets to treat demyelinating disorders. Our study presents the first integrated transcriptional map, to our knowledge, of lncRNA elements at multiple stages during OL lineage progression, and defines the association of distinct OL-expressing lncRNA clusters with corresponding protein-coding genes.

By integrative analyses of transcriptome profiling and genome-wide chromatin states, we systematically constructed and cataloged lncRNAs that are actively transcribed during OL differentiation. Previously, studies used the public datasets of poly-A(+) non-stranded RNAs to identify lncRNAs in OPCs (Dong et al., 2015) and glial cell differentiation from mixed neural progenitors using a microarray platform (Mercer et al., 2010). The lncRNAs annotated in the present de novo annotation not only include lncRNAs previously annotated, but also identify over 500 unique, previously un-annotated lncRNAs that are enriched during OL differentiation. lncRNA expression profiling at multiple phases during OL differentiation and regeneration after spinal cord injury revealed that transcription of lncRNAs, like mRNAs, is dynamically regulated during development and repair. Our analyses reveal tissue and temporal specificity and genetic diversity of complex lncOLs, which allow fine mapping the dynamic processes and functions of lncRNAs in OL development and demyelinating diseases.

The unmapped nature of lncRNAs and their interaction with protein-coding genes during OL lineage progression has represented a substantial obstacle to the full delineation of the transcriptional and epigenetic network that regulates stepwise myelinogenesis. The reconstruction of a conserved co-expression network that links lncRNAs with protein-coding gene expression and their functions allows identifying the potential functions of lncRNAs during OL lineage progression and remyelination.

LncOL1 Is Both Sufficient and Crucial for the Timely Initiation of OL Differentiation and Myelination

The functions of the vast majority of lncRNA transcripts are currently unknown. We identify that *lncOL1* is an evolutionally conserved and OL-restricted lncRNA. Enforced expression of *lncOL1* induces precocious OL formation in the developing brain. Inhibition of *lncOL1* by siRNA silencing in vitro and CRISPR-mediated targeting in vivo establish a critical role of *lncOL1* for the timely initiation of OL myelination. Although myelination recovery is observed in the adult *lncOL1* null mice, this may indicate the functional redundancy of other factors. Indeed, additional silencing of other lncOLs in *lncOL1* knockout OPCs led to a further downregulation of myelin genes in vitro (Figure S7A). Therefore, OL differentiation can proceed at later stages in the absence of *lncOL1*, but at a suboptimal level. The requirement of *lncOL1* for the timely myelination onset is consistent with its upregulation in newly formed myelinating OLs. *lncOL1* may act as a transiently expressed regulator to boost or accelerate the initiation of myelinogenesis, whereas it subsides when myelination falls into a steady maintenance phase in adulthood.

De novo transcriptome reconstruction reveals a cohort of previously un-annotated OL-enriched lncRNAs, including *lncOL4*, which regulates myelin gene expression (Figure 2F). Intriguingly, the miR219-2 gene is located within the intron of *lncOL4*. Given that *lncOL4* knockdown leads to a downregulation of miR-219 and that the potential regulatory region of miR-219 is present in *lncOL4* (Figures S7B and S7C), the function of *lncOL4* in OL differentiation is likely channeled through the control of miR-219, a critical regulator of OL differentiation (Dugas et al., 2010; Zhao et al., 2010). Together, these data suggest that lncRNAs are not simply transcriptional noise resulting from stochastic promoter firing, but rather play an important role in OL differentiation and myelinogenesis, and that individual lncRNAs likely regulate OL differentiation through distinct mechanisms.

LncOL1 Cooperates with a Chromatin-Remodeling Factor Suz12 to Antagonize the Gene Program that Maintains the OL Progenitor State

Epigenetic regulation plays an important role in OL development and myelination (Emery and Lu, 2015). Recent studies have shown that deposition of repressive H3K27me3 marks by the PRC2 complex increases during OL differentiation and contributes to the terminal differentiation of myelinating OLs (Liu et al., 2015; Sher et al., 2012). Our study revealed that *lncOL1* directly interacts with Suz12, a core component of the PRC2 complex for H3K27 methylation. We demonstrated that the Suz12-PRC2 complex is required for OL differentiation through transcriptional silencing of OPC-enriched gene clusters. More importantly, *lncOL1*-driven OL differentiation was diminished by the loss of Suz12 or PRC2 activity, supporting that *lncOL1* exerts its regulatory function through Suz12.

Transcriptome profiling of *lncOL1* null OLs indicated that *lncOL1* perturbation resulted in a derepression of Suz12 target genes in a trans-regulatory manner, suggesting that *lncOL1* is crucial for the repressive activity of the PRC2 complex on Suz12 target gene expression. We further found that *lncOL1* interacts with Suz12 to form a repressor complex to silence gene transcription through implementing repressive H3K27me3 marks on gene regulatory elements. Although further studies will be required to fully elucidate the mechanism behind *lncOL1* function, our work suggests that *lncOL1* promotes OL differentiation, in part, by modulating the recruitment of Suz12 to silence the OPC-enrichment network. Thus, the *lncOL1* interaction with Suz12 forms a repressor complex to control the balance between OPC maintenance and OL differentiation (Figure 7O), suggesting an important role of the interplay between lncRNAs and histone-modifying enzymes in OL development.

lncRNAs in Myelin Repair

Functional studies of lncRNAs in cardiac and liver regeneration indicate that lncRNAs, like microRNAs (miRNAs), likely act as fine-tuning factors that enable cells and organs to respond to stress, injury, and chronic disease (Lorenzen and Thum, 2016). In line with this, our study demonstrates that expression of lncRNAs is dynamically regulated across remyelinating phases. In particular, we showed that *lncOL1* is reactivated and critical for robust OL regeneration after demyelinating injury. The crucial role of *lncOL1* in the regulation of timely OL differentiation and remyelination highlights a therapeutic potential of lncRNAs as a molecular therapy to enhancing myelin regeneration. Given the unique expression pattern of individual lncRNAs in the OL lineage, modulation of OL-restricted

lncRNA expression will not impact other cell types and would provide unique therapeutic avenues for promoting myelin repair in demyelinating diseases, with lower odds of side effects.

Experimental Procedures

Full details are provided in the Supplemental Experimental Procedures. Complete protocols are available upon request from Q.R.L.

Animals

All animal studies were approved by the Institutional Animal Care and Use Committees of the Cincinnati Children's Hospital Medical Center. Further details are described in the Supplemental Experimental Procedures.

Primary OPC Isolation and Culture

Primary rat OPCs were isolated and cultured as described previously (Chen et al., 2007). Mouse OPCs were isolated from P5-P6 cortices by immunopanning, as previously described (Yu et al., 2013). Rat OPCs were transfected with expression vectors or siRNAs using Amaxa Nucleofector (Lonza) according to the manufacturer's protocol. The detailed information for cell culture, immunocytochemistry, qRT-PCR, and western blotting and co-immunoprecipitation assays are described in the Supplemental Experimental Procedures.

lncRNA Assembly and Annotation

Mouse OPCs and OLs were sequenced (paired-end stranded-specific, 80– 90 million reads/sample) in duplicates for ab initio transcriptome assembly with Cufflinks v2.2.1. Briefly, Cufflinks was run with the following options: -u, -N, -g (mm10GTFfile provided as guide), and -M (rRNA and 7SK RNA maskfile provided). We generated transcriptome assemblies for each of these samples separately and then used Cuffmerge to combine all annotations. For all subsequent filtering and processing steps, please see the Supplemental Experimental Procedures.

RNA-Seq and Data Analysis

Total RNA was extracted from samples using the RNeasy Plus mini kit (Life Technologies). The resulting RNA samples were then used as input for library construction with TruSeq Stranded mRNA Library Prep Kit, according to the manufacturer's instructions. All RNA-seq data were aligned to mm10 using TopHat v2.1.0 with default parameters. We used Cuffdiff v1.3 for all differential expression (DE) analyses with our custom annotation containing RefSeq entries plus OL-expressing lncRNAs, as described below. In all DE tests, a gene was considered significant if the fold change was more than 1.5 and the q value was less than 0.05.

ChIP-Seq and Data Analysis

ChIP assays were performed in rat OPCs with antibody against Suz12 (Cell Signaling Technology, #3737), as previously described (Yu et al., 2013). For details, see the Supplemental Experimental Procedures. Sequencing data were aligned to March 2012 rat

genome assembly (rn5) using Bowtie with the following options: -p 8 and -m 1. Resulting SAM files were converted to BAM format using SAM tools. Peak calling was performed using MACS (Model-Based Analysis of ChIP-Seq), with a p value cut off of $1 \times e^{9}$.

Statistical Analysis

All analyses were done using GraphPad Prism 6.00. Data are shown as mean ± SEM or as a box and whisker plot. Data distribution was assumed to be normal, but this was not formally tested. Statistical significance was determined using two-tailed Student's t tests or Wilcoxon rank-sum and signed-rank tests, as indicated. A one-way ANOVA test was performed by multiple comparisons. Significance was set as $*p < 0.05$, $**p < 0.01$, and $***p < 0.001$, unless otherwise indicated. No statistical methods were used to predetermine sample sizes, but our sample sizes are similar to those reported in previous publications. Quantifications were performed from at least three independent experiments. Lysolecithin-induced demyelinating injury was performed in a double-blinded fashion.

Supplementary Material

Refer to Web version on PubMed Central for supplementary material.

Acknowledgments

The authors would like to thank Dr. Noriyoshi Usui for initial characterization of lncRNAs and Zhixing Ma for technical support. We thank Dr. Sung Yoon and Dr. Edward Hurlock for suggestions. This study was funded in part by grants from the National Multiple Sclerosis Society (RG-1507-05671) and NIH (R01NS072427 and R01NS075243) to Q.R.L.

References

Batista PJ, Chang HY. Long noncoding RNAs: cellular address codes in development and disease. Cell. 2013; 152:1298–1307. [PubMed: 23498938]

Bellucci M, Agostini F, Masin M, Tartaglia GG. Predicting protein associations with long noncoding RNAs. Nat Methods. 2011; 8:444–445. [PubMed: 21623348]

Bhan A, Mandal SS. Long noncoding RNAs: emerging stars in gene regulation, epigenetics and human disease. ChemMedChem. 2014; 9:1932–1956. [PubMed: 24677606]

Chang A, Tourtellotte WW, Rudick R, Trapp BD. Premyelinating oligodendrocytes in chronic lesions of multiple sclerosis. N Engl J Med. 2002; 346:165–173. [PubMed: 11796850]

Chen Y, Balasubramaniyan V, Peng J, Hurlock EC, Tallquist M, Li J, Lu QR. Isolation and culture of rat and mouse oligodendrocyte precursor cells. Nat Protoc. 2007; 2:1044–1051. [PubMed: 17546009]

Chen K, Deng S, Lu H, Zheng Y, Yang G, Kim D, Cao Q, Wu JQ. RNA-seq characterization of spinal cord injury transcriptome in acute/ subacute phases: a resource for understanding the pathology at the systems level. PLoS ONE. 2013; 8:e72567. [PubMed: 23951329]

Conway E, Healy E, Bracken AP. PRC2 mediated H3K27 methylations in cellular identity and cancer. Curr Opin Cell Biol. 2015; 37:42–48. [PubMed: 26497635]

Derrien T, Johnson R, Bussotti G, Tanzer A, Djebali S, Tilgner H, Guernec G, Martin D, Merkel A, Knowles DG, et al. The GENCODE v7 catalog of human long noncoding RNAs: analysis of their gene structure, evolution, and expression. Genome Res. 2012; 22:1775–1789. [PubMed: 22955988]

Diederichs S. The four dimensions of noncoding RNA conservation. Trends Genet. 2014; 30:121–123. [PubMed: 24613441]

Dong X, Chen K, Cuevas-Diaz Duran R, You Y, Sloan SA, Zhang Y, Zong S, Cao Q, Barres BA, Wu JQ. Comprehensive identification of long non-coding RNAs in purified cell types from the brain

reveals functional LncRNA in OPC fate determination. PLoS Genet. 2015; 11:e1005669. [PubMed: 26683846]

Doudna JA, Charpentier E. Genome editing. The new frontier of genome engineering with CRISPR-Cas9. Science. 2014; 346:1258096. [PubMed: 25430774]

Dugas M, Weninger F, Merk S, Kohlmann A, Haferlach T. A generic concept for large-scale microarray analysis dedicated to medical diagnostics. Methods Inf Med. 2006; 45:146–152. [PubMed: 16538279]

Dugas JC, Cuellar TL, Scholze A, Ason B, Ibrahim A, Emery B, Zamanian JL, Foo LC, McManus MT, Barres BA. Dicer1 and miR-219 are required for normal oligodendrocyte differentiation and myelination. Neuron. 2010; 65:597–611. [PubMed: 20223197]

Emery B, Lu QR. Transcriptional and epigenetic regulation of oligodendrocyte development and myelination in the central nervous system. Cold Spring Harb Perspect Biol. 2015; 7:a020461. [PubMed: 26134004]

Fatica A, Bozzoni I. Long non-coding RNAs: new players in cell differentiation and development. Nat Rev Genet. 2014; 15:7–21. [PubMed: 24296535]

Franklin RJ, Ffrench-Constant C. Remyelination in the CNS: from biology to therapy. Nat Rev Neurosci. 2008; 9:839–855. [PubMed: 18931697]

Frederick TJ, Wood TL. IGF-I and FGF-2 coordinately enhance cyclin D1 and cyclin E-cdk2 association and activity to promote G1 progression in oligodendrocyte progenitor cells. Mol Cell Neurosci. 2004; 25:480–492. [PubMed: 15033176]

Guttman M, Amit I, Garber M, French C, Lin MF, Feldser D, Huarte M, Zuk O, Carey BW, Cassady JP, et al. Chromatin signature reveals over a thousand highly conserved large non-coding RNAs in mammals. Nature. 2009; 458:223–227. [PubMed: 19182780]

Hajarnis SS, Patel V, Aboudehen K, Attanasio M, Cobo-Stark P, Pontoglio M, Igarashi P. Transcription factor hepatocyte nuclear factor-1b (HNF-1b) regulates microRNA-200 expression through a long non-coding RNA. J Biol Chem. 2015; 290:24793–24805. [PubMed: 26292219]

Kong L, Zhang Y, Ye ZQ, Liu XQ, Zhao SQ, Wei L, Gao G. CPC: assess the protein-coding potential of transcripts using sequence features and support vector machine. Nucleic Acids Res. 2007; 35:W345–W349. [PubMed: 17631615]

Konze KD, Ma A, Li F, Barsyte-Lovejoy D, Parton T, Macnevin CJ, Liu F, Gao C, Huang XP, Kuznetsova E, et al. An orally bioavailable chemical probe of the lysine methyltransferases EZH2 and EZH1. ACS Chem Biol. 2013; 8:1324–1334. [PubMed: 23614352]

Lalevée S, Feil R. Long noncoding RNAs in human disease: emerging mechanisms and therapeutic strategies. Epigenomics. 2015; 7:877–879. [PubMed: 26418705]

Lin MF, Jungreis I, Kellis M. PhyloCSF: a comparative genomics method to distinguish protein coding and non-coding regions. Bioinformatics. 2011; 27:i275–i282. [PubMed: 21685081]

Liu J, Magri L, Zhang F, Marsh NO, Albrecht S, Huynh JL, Kaur J, Kuhlmann T, Zhang W, Slesinger PA, et al. Chromatin landscape defined by repressive histone methylation during oligodendrocyte differentiation. J Neurosci. 2015; 35:352–365. [PubMed: 25568127]

Ljungberg P, Rapola J, Holmberg C, Holthöfer H, Jalanko H. Glomerular anionic charge in congenital nephrotic syndrome of the Finnish type. Histochem J. 1995; 27:536–546. [PubMed: 7591846]

Lopez-Anido, C., Sun, G., Koenning, M., Srinivasan, R., Hung, HA., Emery, B., Keles, S., Svaren, J. Differential Sox10 genomic occupancy in myelinating glia. Glia. 2015. Published online May 14, 2015. http://dx.doi.org/10.1002/glia.22855

Lorenzen JM, Thum T. Long noncoding RNAs in kidney and cardiovascular diseases. Nat Rev Nephrol. 2016; 12:360–373. [PubMed: 27140855]

Lu F, Chen Y, Zhao C, Wang H, He D, Xu L, Wang J, He X, Deng Y, Lu EE, et al. Olig2-dependent reciprocal shift in PDGF and EGF receptor signaling regulates tumor phenotype and mitotic growth in malignant glioma. Cancer Cell. 2016; 29:669–683. [PubMed: 27165742]

Maass PG, Luft FC, Bähring S. Long non-coding RNA in health and disease. J Mol Med (Berl). 2014; 92:337–346. [PubMed: 24531795]

Mar S, Noetzel M. Axonal damage in leukodystrophies. Pediatr Neurol. 2010; 42:239–242. [PubMed: 20304325]

Mercer TR, Qureshi IA, Gokhan S, Dinger ME, Li G, Mattick JS, Mehler MF. Long noncoding RNAs in neuronal-glial fate specification and oligodendrocyte lineage maturation. BMC Neurosci. 2010; 11:14. [PubMed: 20137068]

Mitsui Y, Chang I, Fukuhara S, Hiraki M, Arichi N, Yasumoto H, Hirata H, Yamamura S, Shahryari V, Deng G, et al. CYP1B1 promotes tumorigenesis via altered expression of CDC20 and DAPK1 genes in renal cell carcinoma. BMC Cancer. 2015; 15:942. [PubMed: 26626260]

Quinn JJ, Chang HY. Unique features of long non-coding RNA biogenesis and function. Nat Rev Genet. 2016; 17:47–62. [PubMed: 26666209]

Ramos AD, Diaz A, Nellore A, Delgado RN, Park KY, Gonzales-Roybal G, Oldham MC, Song JS, Lim DA. Integration of genome-wide approaches identifies lncRNAs of adult neural stem cells and their progeny in vivo. Cell Stem Cell. 2013; 12:616–628. [PubMed: 23583100]

Ratajczak MZ. Igf2-H19, an imprinted tandem gene, is an important regulator of embryonic development, a guardian of proliferation of adult pluripotent stem cells, a regulator of longevity, and a 'passkey' to cancerogenesis. Folia Histochem Cytobiol. 2012; 50:171–179. [PubMed: 22763974]

Rinn JL, Chang HY. Genome regulation by long noncoding RNAs. Annu Rev Biochem. 2012; 81:145–166. [PubMed: 22663078]

Sher F, Boddeke E, Olah M, Copray S. Dynamic changes in Ezh2 gene occupancy underlie its involvement in neural stem cell self-renewal and differentiation towards oligodendrocytes. PLoS ONE. 2012; 7:e40399. [PubMed: 22808153]

Shi J, Wang E, Zuber J, Rappaport A, Taylor M, Johns C, Lowe SW, Vakoc CR. The polycomb complex PRC2 supports aberrant self-renewal in a mouse model of MLL-AF9;Nras(G12D) acute myeloid leukemia. Oncogene. 2013; 32:930–938. [PubMed: 22469984]

Trapnell C, Williams BA, Pertea G, Mortazavi A, Kwan G, van Baren MJ, Salzberg SL, Wold BJ, Pachter L. Transcript assembly and quantification by RNA-seq reveals unannotated transcripts and isoform switching during cell differentiation. Nat Biotechnol. 2010; 28:511–515. [PubMed: 20436464]

Trapp BD, Peterson J, Ransohoff RM, Rudick R, Mörk S, Bö L. Axonal transection in the lesions of multiple sclerosis. N Engl J Med. 1998; 338:278–285. [PubMed: 9445407]

Ulitsky I, Bartel DP. lincRNAs: genomics, evolution, and mechanisms. Cell. 2013; 154:26–46. [PubMed: 23827673]

van Dongen S, Abreu-Goodger C. Using MCL to extract clusters from networks. Methods Mol Biol. 2012; 804:281–295. [PubMed: 22144159]

Wang L, Park HJ, Dasari S, Wang S, Kocher JP, Li W. CPAT: Coding-Potential Assessment Tool using an alignment-free logistic regression model. Nucleic Acids Res. 2013; 41:e74. [PubMed: 23335781]

Weng Q, Chen Y, Wang H, Xu X, Yang B, He Q, Shou W, Chen Y, Higashi Y, van den Berghe V, et al. Dual-mode modulation of Smad signaling by Smad-interacting protein Sip1 is required for myelination in the central nervous system. Neuron. 2012; 73:713–728. [PubMed: 22365546]

Yu Y, Chen Y, Kim B, Wang H, Zhao C, He X, Liu L, Liu W, Wu LM, Mao M, et al. Olig2 targets chromatin remodelers to enhancers to initiate oligodendrocyte differentiation. Cell. 2013; 152:248–261. [PubMed: 23332759]

Yue F, Cheng Y, Breschi A, Vierstra J, Wu W, Ryba T, Sandstrom R, Ma Z, Davis C, Pope BD, et al. A comparative encyclopedia of DNA elements in the mouse genome. Nature. 2014; 515:355–364. [PubMed: 25409824]

Zhang Y, Jalili F, Ouamara N, Zameer A, Cosentino G, Mayne M, Hayardeny L, Antel JP, Bar-Or A, John GR. Glatiramer acetate-reactive T lymphocytes regulate oligodendrocyte progenitor cell number in vitro: role of IGF-2. J Neuroimmunol. 2010; 227:71–79. [PubMed: 20637510]

Zhang Y, Chen K, Sloan SA, Bennett ML, Scholze AR, O'Keeffe S, Phatnani HP, Guarnieri P, Caneda C, Ruderisch N, et al. An RNA-sequencing transcriptome and splicing database of glia, neurons, and vascular cells of the cerebral cortex. J Neurosci. 2014; 34:11929–11947. [PubMed: 25186741]

Zhao X, He X, Han X, Yu Y, Ye F, Chen Y, Hoang T, Xu X, Mi QS, Xin M, et al. MicroRNA-mediated control of oligodendrocyte differentiation. Neuron. 2010; 65:612–626. [PubMed: 20223198]

Zhao C, Deng Y, Liu L, Yu K, Zhang L, Wang H, He X, Wang J, Lu C, Wu LN, et al. Dual regulatory switch through interactions of Tcf7l2/ Tcf4 with stage-specific partners propels oligodendroglial maturation. Nat Commun. 2016; 7:10883. [PubMed: 26955760]

Zuchero JB, Barres BA. Intrinsic and extrinsic control of oligodendrocyte development. Curr Opin Neurobiol. 2013; 23:914–920. [PubMed: 23831087]

Highlights

- Transcriptome reconstruction reveals a dynamic network of lncRNAs in oligodendrocytes
- Identification of oligodendrocyte-enriched lncOLs critical for OPC differentiation
- Oligodendrocyte-restricted lncOL1 regulates timely CNS myelination and remyelination
- lncOL1 interacts with Suz12-PRC2 complex to orchestrate OPC differentiation program

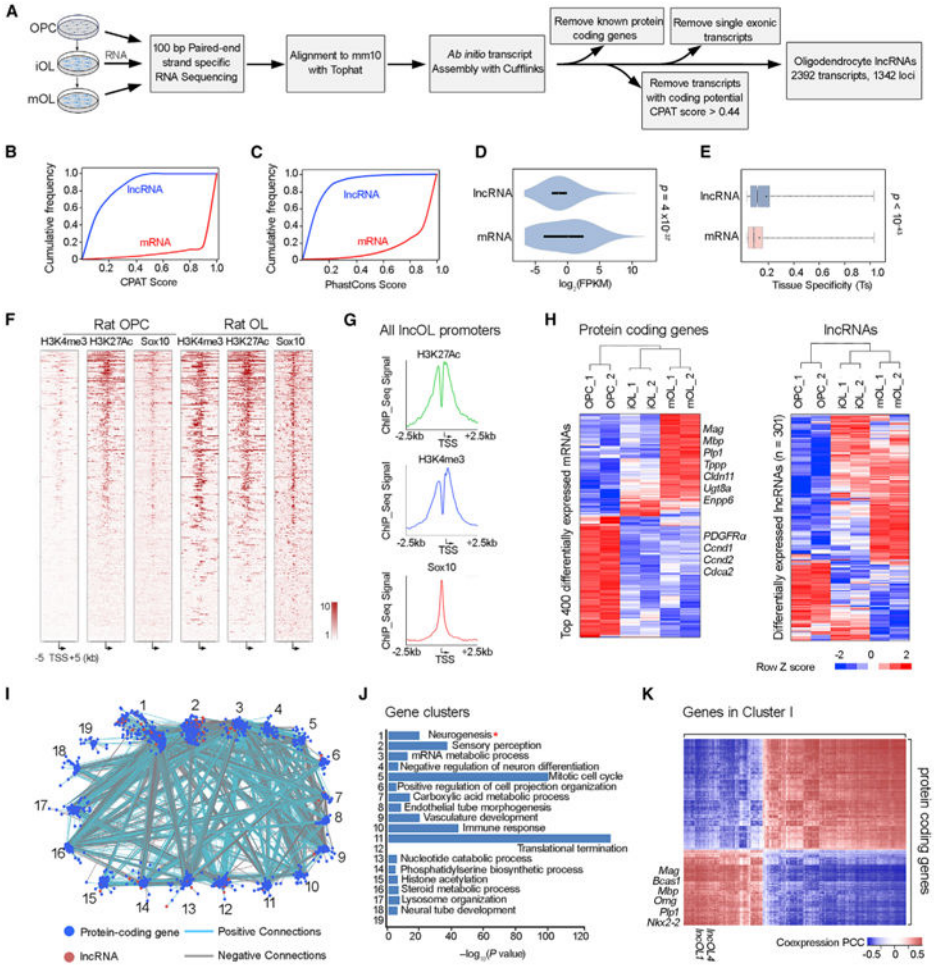

Figure 1. De Novo Mapping of lncRNA Transcriptome in OL Lineage Cells

(A) Schematic procedure for discovering lncRNAs in primary mouse OPCs and OLs.

(B) Cumulative frequency plot of coding potential CPAT scores for mRNA and lncRNA genes.

(C) Cumulative frequency plot of PhastCons conservation scores for mRNA and lncRNA genes.

(D) Violin plot of $\log_2$ maximum expression values (FPKM, fragments per kilobase of transcript per million mapped reads) for mRNA and lncRNA genes. Student's t test with Welch's corrections.

(E) Box plot of tissue specificity index (Ts score) for mRNA and lncRNA genes. Ts scores are calculated by analysis of fractional expression in OLs across all the tissues examined. Whiskers show the minimum and maximum, and boxes extend from the first to the third quartiles, with cross lines at the medians; Student's t test with Welch's corrections.

(F) Heat map representation of ChIP-seq signal density for H3K4me3, H3K27ac, and Sox10 for 5 kb centered on predicted lncRNA TSSs in rat OPCs and OLs.

(G) Histogram depicting ChIP-seq signal density on all predicted lncRNA promoters for H3K27ac, H3K4me3, and Sox10 in primary rat OLs.

(H) Heat maps showing top differentially expressed protein coding (left) and lncRNA (right) genes during mouse OPC maturation.
(I) Cytoscape representation of the 19 largest MCL clusters in the lncOL and protein-coding gene co-expression network from all tissues and cells examined.
(J) GO enrichment for the 19 largest MCL clusters. The most significant GO categories are displayed.
(K) Heat map displaying Pearson correlation coefficients of lncOL and protein-coding genes in MCL cluster I. Columns and rows represent protein-coding genes and lncRNAs, respectively. Myelin-associated genes and lncOLs are highly correlated.

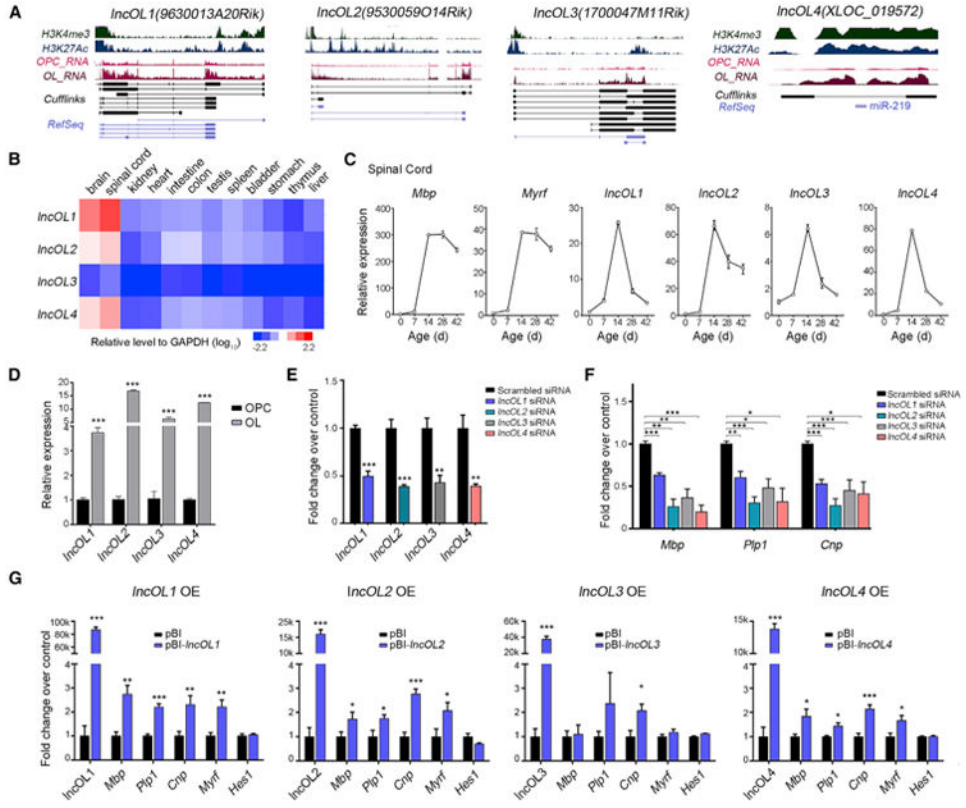

Figure 2. OL-Enriched lncRNAs Regulate OL Differentiation

(A) UCSC genome browser tracks of *lncOL1–4* loci depict RNA-seq signals for OPCs and OLs, along with ChIP-seq signals for H3K4me3 and H3K27ac. Bottom tracks depict de novo transcript models created from Cufflinks and RefSeq annotations.

(B) qRT-PCR analyses of *lncOL1–lncOL4* levels in different murine tissues at P14.

(C) qRT-PCR analyses of *Mbp*, *Myrf*, and *lncOL1–lncOL4* transcript levels in mouse spinal cords at indicated stages. Data are presented as mean ± SEM, n = 3 animals at each time point.

(D) qPCR analyses for *lncOL1–lncOL4* in primary mouse OPCs and OLs. Data are presented as mean ± SEM, n = 3 independent experiments; ***p < 0.001; paired Student's t test.

(E) qPCR validation of efficiency of siRNA knockdown of lncRNAs. Data are presented as mean ± SEM; n = 4 independent experiments, **p < 0.01, ***p < 0.001;paired Student's t test.

(F) qRT-PCR analyses of OL-differentiation-associated genes following treatments with scrambled or lncRNA-targeted siRNAs. Data are presented as mean ±SEM; n = 4 independent experiments, *p < 0.05, **p < 0.01, ***p < 0.001; one-way ANOVA with post hoc Tukey's test.

(G) qRT-PCR analyses of OL-differentiation associated genes in rat OLs transduced with control or lncRNA-overexpressing vectors. Data are presented as mean ± SEM; n = 4 independent experiments, *p < 0.05, **p < 0.01, ***p < 0.001; paired Student's t test.

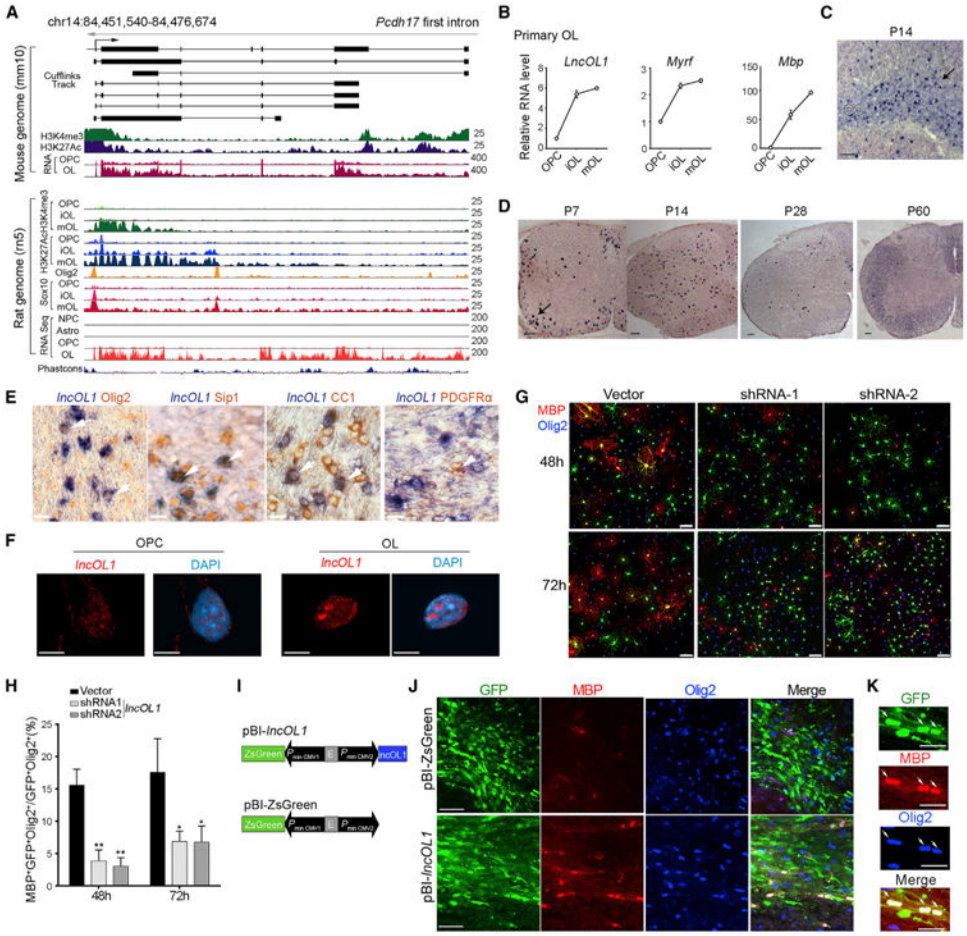

Figure 3. *lncOL1* Is a Conserved OL-Specific lncRNA that Regulates OPC Differentiation

(A) Genome browser tracks of the *lncOL1* locus in mouse OLs (top) and its corresponding genomic locus in rat OLs (bottom). Top tracks depict RNA-seq signals for mouse OPCs and OLs and ChIP-seq signals for H3K4me3 and H3K27ac (Lu et al., 2016). Bottom tracks represent RNA-seq signals for rat OPCs, OLs, astrocytes (Astro), and neural precursor cells (NPCs) and ChIP-seq signals for H3K4me3, H3K27ac, Olig2, and Sox10 in rat OPCs and OLs.

(B) qRT-PCR analyses of *lncOL1*, *Myrf*, and *Mbp* transcripts in primary mouse OPCs, iOLs, and mOLs. Data are presented as mean ± SEM, n = 3 at each timepoint.

(C and D) In situ hybridization showing expression of *lncOL1* in the cerebral white matter (C) and spinal cord (D) at the indicated time points. Arrows point to *lncOL1*-expressing cells. CC, corpus callosum. Scale bar, 100 μm.

(E) In situ hybridization for *lncOL1* (blue) and immunohistochemistry for Olig2, Sip1/Zeb2, CC1, or PDGFRα (brown) at P14. Arrows indicate *lncOL1*$^{+}$ cells. Arrowheads indicate PDGFRα^{+} OPCs without *lncOL1* expression. Scale bar, 10 μm.

(F) FISH for *lncOL1* in primary OPCs and OLs differentiated for 3 days. Nuclei are counterstained with DAPI. Scale bar, 5 μm.

(G) Immunostaining for MBP and Olig2 after 48 or 72 hr of differentiation after PDGFAA withdrawal in control or *lncOL1*-shRNA transduced mouse OLs. Scale bar, 50 μm.

(H) Histogram depicting the percentage of MBP^+ cells among GFP^+ transduced cells. Data are presented as mean ± SEM; n = 3 independent experiments; *p < 0.05, **p < 0.01; one-way ANOVA with post hoc Tukey's test.
(I) Schematic presentation of control and *lncOL1*-overexpressing vectors used for in utero electroporation. *lncOL1* transcription is driven by bidirectional promoters in pBI.
(J and K) Cortical sections at E17.5, 3 days after electroporation with control (pBI-zsgreen) or *lncOL1* overexpressing (pBI-*lncOL1*/Zsgreen) vectors. (K) shows high magnification of transduced cells co-labeled with GFP, MBP, and Olig2. Scale bars in (J), 50 mm; scale bars in (K), 25 μm.

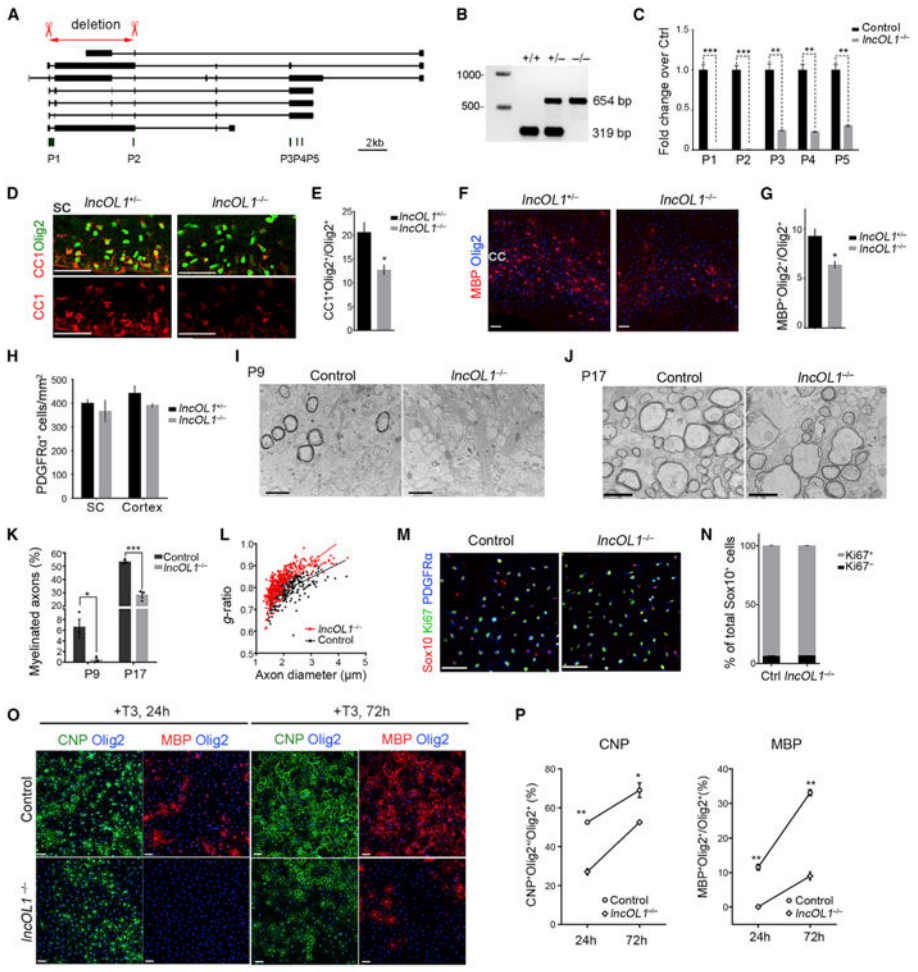

Figure 4. *lncOL1*-Deficient Mice Exhibit Defects in the Onset of OL Differentiation and Myelination

(A) CRISPR/Cas9-mediated knockout at the *lncOL1* locus. Two sgRNA recognition sites for *lncOL1* deletion are demarcated in red. Primer pairs 1–5 (P1–P5) were used for qRT-PCR analysis of knockout in different *lncOL1* exons.

(B) Validation of *lncOL1*-KO mouse lines by PCR genotyping. Wild-type allele: 319 bp; mutant allele: 654 bp.

(C) qPCR analyses of *lncOL1* transcript levels with primer pairs P1–P5 in brains from *lncOL1*-KO and control littermates at P12. Data are presented as mean ±SEM; n = 3 animals; **p < 0.01, ***p < 0.001; Student's t test.

(D) The spinal white matter at P1 from control and *lncOL1* null animals was co-immunostained for CC1 and Olig2. Scale bar, 50 μm.

(E) Quantification of $CC1^+$OLs as a percentage of total $Olig2^+$ cells in control and *lncOL1*-KO spinal cords at P1. Data are presented as mean ± SEM;n =3animals;*p < 0.05; Student's t test.

(F) Immunofluorescence labeling for Olig2 and MBP in control and *lncOL1*-KO corpus callosum at P6. Scale bars, 50 μm.

(G) Quantification of MBP^+ OLs as a percentage of all $Olig2^+$ cells within the corpus callosum of control and *lncOL1-KO* mice at P6. Data are presented as mean ± SEM; n = 4 animals; *p < 0.05; Student's t test.
(H) Quantification of $PDGFR\alpha^+$ OPC density in control and *lncOL1-KO* brains (Br) and spinal cords (SC). Data are presented as mean ± SEM; n = 3 to 4 animals.
(I and J) Representative electron micrographs of transverse optic nerve sections from control and *lncOL1* -KO animals at P9 (I) and P17 (J). Scale bar, 2 μm.
(K) Quantification of the percentage of axons myelinated at P9 and P17. Data are presented as mean ± SEM; each data point is an average for a single animal; n = 4 animals; *p < 0.05, ***p < 0.001; Student's t test.
(L) Scatter plots of *g*-ratios of individual fibers from *lncOL1* -KO and littermate controls at P17. Between 300 and 400 axons from three mice of each genotype were analyzed; ***p < 0.001.
(M) Immunostaining for Ki67, Sox10, and PDGFRα on control and *lncOL1* null OPCs cultured with PDGFAA. Scale bar, 50 μm.
(N) Percentage of $Ki67^+$ proliferating and $Ki67^-$ non-proliferating OPCs among $Sox10^+$ $PDGFR\alpha^+$OPCs from control *or lncOL1* null mice. Data are presented as mean ± SEM; n = 3 independent experiments.
(O) Immunostaining for MBP, CNP, and Olig2 on mouse OPCs from control and *lncOL1* null mice. Cells differentiated with T3 for 24 and 72 hr are shown. Scale bar, 50 μm.
(P) The proportions of CNP^+ (left) or MBP^+ (right) OLs in mouse OL cultures from control and *lncOL1* null mice. Data are presented as mean ± SEM; n = *2*–4 independent experiments; *p < 0.005, **p < 0.01; one-way ANOVA with post hoc Tukey's test.

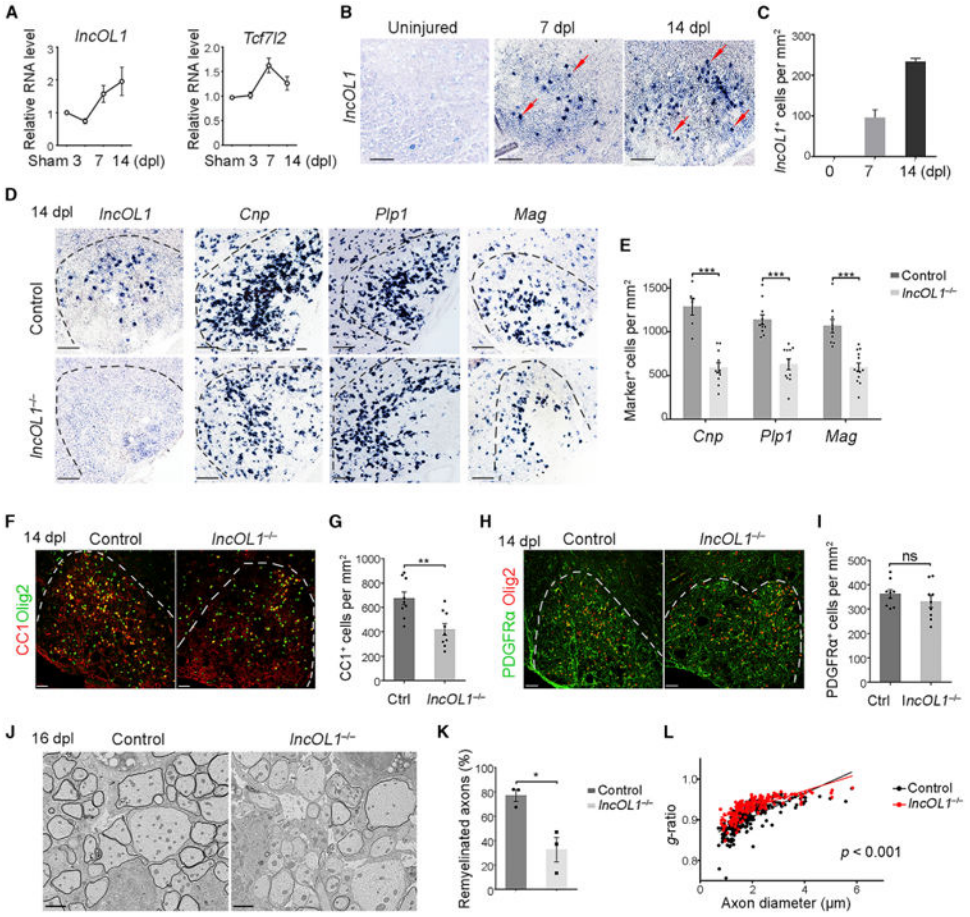

Figure 5. *lncOL1* Is Critical for Proper Myelin Repair after Demyelination

(A) qRT-PCR analyses for *lncOL1* and *Tcf7l2* levels in spinal cord lesions at various time points post LPC-induced demyelination. Data are presented as mean ± SEM; n = 4 animals at each time point.

(B) In situ hybridization for *lncOL1* in representative spinal cord lesions from 8-week-old wild-type control mice at 7 and 14 dpl. Scale bars, 100 μm.

(C) Quantification of *lncOL1*-expressing cells in unlesioned and lesioned regions of spinal cords of wild-type control mice at 7 and 14 dpl. Data are presented as mean ± SEM; n = 3; Student's t test.

(D) In situ hybridization for *lncOL1*, *Plp*, *Cnp*, and *Mag* in representative spinal cord lesions from control and *lncOL1*-KO mice at 14 dpl. Scale bars, 100 μm.

(E) Quantification of mature OLs in 14 dpl demyelinated spinal cord of *lncOL1* null and control mice. Data are presented as mean ± SEM; n = 9, ***p < 0.001; Student's t test.

(F) Immunostaining for CC1 and Olig2 in representative spinal cord lesions from control and *lncOL1*-KO mice at 14 dpl. Scale bar, 100 μm.

(G) Quantification of $CC1^+$ OLs in lesions at 14 dpl. Data are presented as mean ± SEM; n = 9, **p < 0.01; Student's t test.

(H) Immunostaining for PDGFRα and Olig2 in representative LPC-induced lesions from control and *lncOL1*-KO mice at 14 dpl. Scale bar, 100 μm.

(I) Quantification of PDGFRα$^+$ OPCs in lesions at 14 dpl. Data are presented as mean ± SEM; n = 9.
(J) Representative electron microscopy images of LPC-induced lesions from control and *lncOL1*-KO mice at 16 dpl. Scale bar, 2 μm.
(K) The percentage of remyelinated axons in LPC-induced lesions of control and *lncOL1*-KO mice at 16 dpl. Data are presented as mean ± SEM; n = 3, *p < 0.05; Student's t test.
(L) The myelin g-ratio in LPC-induced lesions of control and *lncOL1*-KO mice at 16 dpl. n = 3 animals/genotype, p < 0.001; Student's t test.

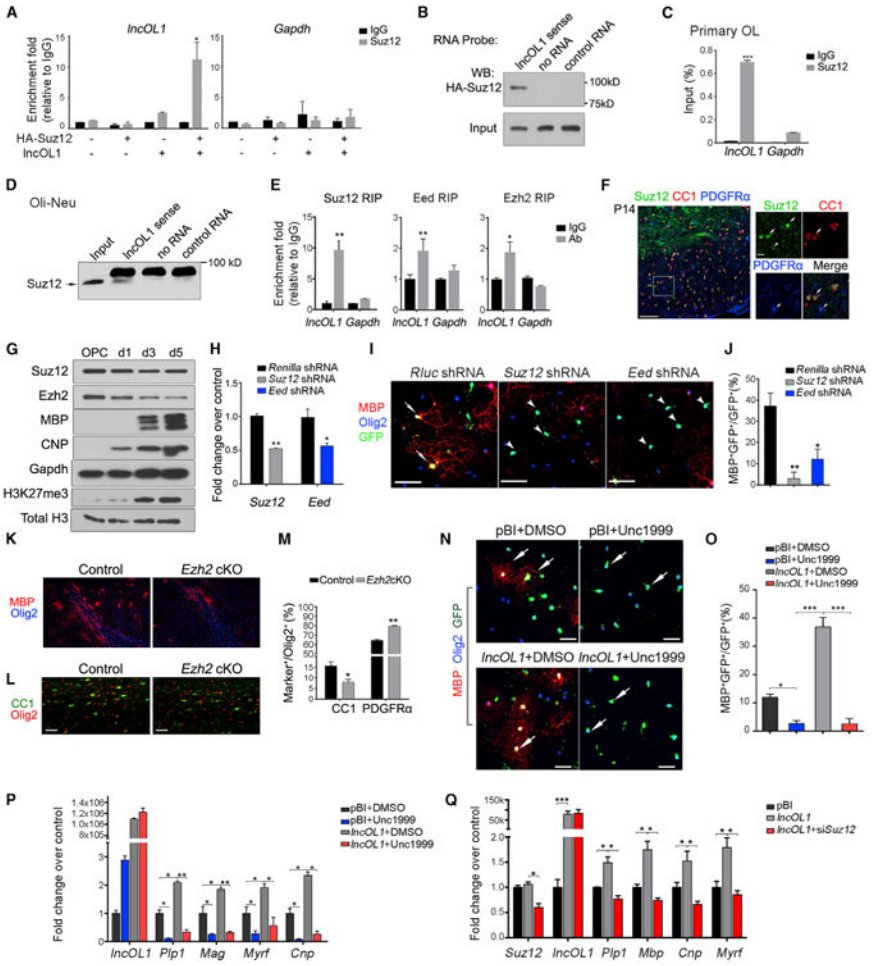

Figure 6. *lncOL1* Interacts with Suz12/PRC2 Complex to Regulate OL Differentiation

(A) HEK293T cells overexpressing HA-tagged Suz12 and pBI-*lncOL1* were lysed and precipitated with anti-Suz12 and control IgG, and analyzed by qRT-PCR for *lncOL1* and *Gapdh*. Data are presented as mean ± SEM; n = 3 independent experiments. *p < 0.05; Student's t test.

(B) Immunoblot for HA-Suz12 after RNA pull-down with biotin-labeled *lncOL1* RNA or biotin-labeled control RNA (*Bmp4*). Pull-down by streptavidin magnetic beads with no RNA probe was used as negative control.

(C) qRT-PCR quantification of *lncOL1* and *Gapdh* in Suz12 immunoprecipitates from mouse OLs. Data are presented as mean ± SEM; n = 3 independent experiments. ***p < 0.001; Student's t test.

(D) Immunoblot for endogenous Suz12 in differentiating Oli-Neu cells after RNA pull-down with biotin-labeled *lncOL1* or biotin-labeled control RNA (*Bmp4*). Pulldown by streptavidin beads without RNA probe as a negative control. The larger band appeared as a non-specific protein associated with beads.

(E) qRT-PCR quantification of *lncOL1* and *Gapdh* in Suz12, Eed, and Ezh2 immunoprecipitates using RNA immunoprecipitation (RIP) assay from differentiating oligodendroglial cells (Oli-Neu). Data are presented as mean ± SEM; n = 3 to 4 independent experiments. *p < 0.05, **p < 0.01; Student's t test.

(F) P14 mouse spinal cord transverse sections immunostained for Suz12, CC1, and PDGFRα. Scale bar, 100 μm. Boxed area is shown at higher magnification on right; scale bar, 20 μm.

(G) Immunoblotting for indicated proteins in rat OPCs at 0, 1, 3, and 5 days of culture under differentiation conditions.

(H) qRT-PCR analyses of *Suz12* and *Eed* in Oli-Neu cells transduced with retroviral vectors for expression of shRNAs targeting Renilla luciferase (Rluc) as a control (Ctrl), Suz12, or Eed. Data are presented as mean ± SEM; n = 3, *p < 0.05, **p < 0.01; Student's t test.

(I) Immunostaining for MBP and Olig2 after 72 hr of differentiation induced by T3 in GFP^+ mouse OPCs transduced with retroviral vectors for expression of shRNAs targeting Renilla luciferase, Suz12, or Eed. White arrows indicate control transfected MBP^+ OLs; arrowheads indicate shSuz12- or shEed-transduced cells, respectively. Scale bar, 50 μm.

(J) The percentage of MBP^+ among GFP^+ transduced cells. Data are presented as mean ± SEM; n = 3 independent experiments; *p < 0.05, **p < 0.01; one-way ANOVA with post hoc Tukey's test.

(K and L) Immunofluorescence labeling for Olig2 and MBP (K) or CC1 (L) in the control and *Ezh2*cKO corpus callosum at P7. Scale bars, 50 μm.

(M) Percentage of $CC1^+$ OLs and $PDGFR\alpha^+$ OPCs among $Olig2^+$ cells in P7 control and *Ezh2*cKO corpus callosum. Data are presented as mean ± SEM; n = 2–4 animals; *p < 0.05, **p < 0.01; Student's t test.

(N) Immunostaining for MBP and Olig2 after 72-hr differentiation after PDGFAA withdrawal. DMSO or 1mM Unc1999 were added to culture medium as indicated. Scale bar, 25 μm.

(O) Histogram depicting the percentage of MBP^+ cells among GFP^+ cells. Data are presented as mean ± SEM; n = 4 independent experiments; *p < 0.05, ***p < 0.001; one-way ANOVA with post hoc Tukey's test.

(P) qRT-PCR analyses of OL-differentiation associated genes in rat OLs transduced with control or *lncOL1*-overexpressing vectors in the absence or presence of 1μM Unc1999. Data are presented as mean ± SEM; n = 4 independent experiments; *p < 0.05, **p < 0.01; one-way ANOVA with post hoc Tukey's test.

(Q) qRT-PCR of myelin-associated gene expression in OLs transduced with *lncOL1*-overexpressing vectors with or without siRNAs against *Suz12*. Data are presented as mean ± SEM; n = 4 independent experiments. *p < 0.05; ***p < 0.001; one-way ANOVA with post hoc Tukey's test.

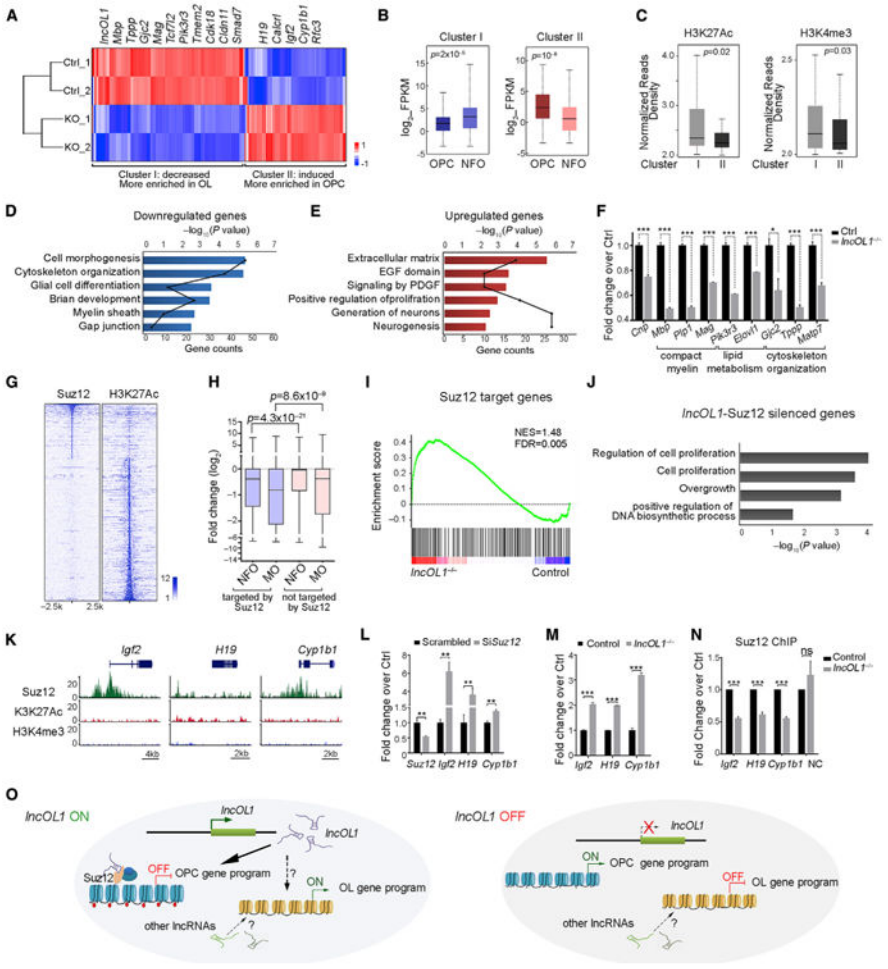

Figure 7. *lncOL1* Acts as a Modulatory Factor for Suz12 to Regulate Transcriptome Dynamics during OL Differentiation

(A) A heat map showing genes differentially expressed in control and *lncOL1* null OLs cultured under differentiation conditions for 24 hr. Modules I and II represent upregulated and downregulated genes compared to wild-type, respectively. Data are from two separate cultures.

(B) Box plots for mRNA levels of module I and II genes in OPCs and newly formed OLs (NFOs).

(C) Box plots comparing the levels of active histone marks H3K27ac and H3K4me3 in the promoters of the genes downregulated (module I) and upregulated (module II) in *lncOL1* null OL lineage cells.

(D and E) GO biological process terms enriched among mRNA genes that show significantly decreased (D) or increased (E) expression upon *lncOL1* deletion relative to control.

(F) qRT-PCR analyses of genes involved in different regulatory arms of OL differentiation. Data are presented as mean ± SEM; n = 3; *p < 0.05, ***p < 0.001; Student's t test.

(G) ChIP-seq density heat maps for Suz12 and H3K27ac within 2.5 kb on either side of the Suz12 and H3K27ac peak centers in OPCs. The sites are ranked in descending order of Suz12 intensity.

(H) Box plots for $\log_2$ fold change in expression levels of the genes targeted with or without Suz12 in NFOs and myelinating OLs (MOs) (Zhang et al., 2014) compared to OPCs.
(I) Gene signature enrichment analysis plot comparing the Suz12-targeted genes (top 500 genes with Suz12-binding peak within ± 50 kb around TSS) in wild-type or *lncOL1*-KO mouse OLs. NES, normalized enrichment score. FDR, false discovery rate.
(J) GO biological process terms enriched among mRNA genes that are targeted by Suz12, with significantly higher expression levels in *lncOL1* null OLs.
(K) Genome browser tracks over select gene loci with ChIP-seq density mapping of Suz12, H3K27ac, and H3K4me3 from rat OLs.
(L) qRT-PCR analyses of Cyp1b1, H19, and Igf2 in control and *lncOL1*-KO OLs. Data are presented as mean± SEM; n =3independent experiments, ***p < 0.001; Student's t test.
(M) qRT-PCR analyses of *Suz12*, *Cyp1b1*, *H19*, and *Igf2* in primary mouse OLs treated with scrambled or Suz12-targeted siRNAs. Data are presented as mean ± SEM; n = 5 independent experiments. **p < 0.01; Student's t test.
(N) ChIP-qPCR analyses for Suz12 at the promoters of *Igf2*, *H19*, and *Cyp1b1* loci or control genomic regions (NC) in primary mouse OLs from control and *lncOL1* knockout animals. Data are presented as mean ± SEM; n = 3 independent experiments. ***p < 0.001; Student's t test.
(O) Schematic diagram for the *lncOL1*-mediated control of OL differentiation. When *lncOL1* expression is turned on, it associates with Suz12-mediated PRC2 complex and silences the OPC gene regulatory program that antagonizes their differentiation process, and thereby allows the activation of the OL differentiation program. When *lncOL1* expression is off, the OPC-promoting gene program is de-repressed and activated, which inhibits OL differentiation processes. Other lncRNAs may cooperate with *lncOL1* to regulate the OL differentiation process. In box plots (B), (C), and (H), whiskers show the minimum and maximum, and boxes extend from the first to the third quartiles, with cross lines at the medians; Mann-Whitney-Wilcoxon test.